Quasiparticle spectrum in superconducting $YBa_2Cu_3O_7$

G. L. Zhao, D. A. Browne, and J. Callaway*
Department of Physics and Astronomy, Louisiana State University, Baton Rouge, Louisiana 70803-4001
(Received 28 July 1995)

We have used the real-axis Eliashberg equations for an anisotropic superconductor to study the quasiparticle density of states of superconducting $YBa_2Cu_3O_7$ in a temperature range from 0 up to 120 K. A first-principles electronic structure and a nonorthogonal tight-binding method was used to calculate the electron-phonon interaction. The large variation we found in gap energies for different bands and directions on the Fermi surface and strong frequency dependence of the gap explains broad features seen in the low temperature tunneling density of states as well as structure seen close to T_c. Above 50 K we have evidence for a gapless superconductor with s-wave pairing.

I. INTRODUCTION

The quasiparticle density of states in high-T_c superconductors has been extensively studied by tunneling experiments[1–7] and photoemission measurements.[8–14] Because of the importance in these materials of the condition of the surface, the short coherence length, and anisotropy, the experimental results are far more complex and much more difficult to understand than for conventional low-T_c superconductors. As a result, it has been difficult to provide experimental confirmation for any of the large number of theories that have been proposed to explain these materials. It is our view that many experimental results cannot be understood without accounting for the very complex band structure and electron-phonon coupling and large number of phonon modes in these materials.

In previous work,[15] two of us used the strong coupling theory of superconductivity and a nonorthogonal tight-binding approach for the calculation of electron-phonon interaction to calculate the transition temperature T_c and the zero-temperature anisotropic superconducting gap function $\Delta(k)$ for $YBa_2Cu_3O_7$ (YBCO). We found a value for T_c that was close to the experimental value and varied only slightly with the value of the Coulomb pseudopotential μ^*; we found a T_c of 89 K for $\mu^*=0.1$ and 92 K for $\mu^*=0.0$. We also found that the superconducting energy gap in YBCO is quite anisotropic, with gap values varying from 10 to 25 meV for different points on the Fermi surface.

The present work extends this earlier calculation[15] to study the temperature dependence of the quasiparticle density of states (DOS) in YBCO between 0 and 120 K. Our results for the quasiparticle DOS at different points of the Fermi surface are consistent with angle-resolved photoemission measurements, while the Fermi surface average of the DOS can explain most of the features seen in tunneling experiments. The only major feature that we do not reproduce is the zero-bias anomaly. In particular, our results show that, unlike conventional superconductors, the strong frequency dependence of the gap leads to noticeable structure in the quasiparticle spectrum even close to T_c, in accord with observations.

In Sec. II of this paper we discuss our method of solving the Eliashberg equations using a first-principles band structure and electron-phonon interaction. In Sec. III we discuss our results for the quasiparticle DOS and compare our results with tunneling experiments. Section IV contains our conclusions.

II. CALCULATION

Our calculation of the superconducting properties is based on solving the temperature dependent Eliashberg gap equation on real axis for an anisotropic superconductor. Because of the anisotropy and the presence of several bands near the Fermi surface, the gap function $\Delta_m(\vec{k},\omega)$ and renormalization function $Z_m(\vec{k},\omega)$ depend on the band index m and momentum $\vec{k}$ in addition to the frequency ω. The Eliashberg equations for $Z_m(\vec{k},\omega)$ and $\Delta_m(\vec{k},\omega)$ are

$$[1-Z_m(\vec{k},\omega)]\omega=\int_0^{\omega_c}d\omega'\sum_{m'}\int dS_{m',\vec{k}'}F^{-}_{m\vec{k}\omega,m'\vec{k}'\omega'}\,\mathrm{Re}\left[\frac{\omega'}{\sqrt{\omega'^2-\Delta^2_{m'}(\vec{k}',\omega')}}\right],$$

$$\Delta_m(\vec{k},\omega)Z_m(\vec{k},\omega)=\int_0^{\omega_c}d\omega'\sum_{m'}\int dS_{m',\vec{k}'}F^{+}_{m\vec{k}\omega,m'\vec{k}'\omega'}\,\mathrm{Re}\left[\frac{\Delta_{m'}(\vec{k}',\omega')}{\sqrt{\omega'^2-\Delta^2_{m'}(\vec{k}',\omega')}}\right]$$

$$-U\int_0^{\omega_c}d\omega'\sum_{m'}\int dS_{m',\vec{k}'}[1-f(\omega')]\mathrm{Re}\left[\frac{\Delta_{m'}(\vec{k}',\omega')}{\sqrt{\omega'^2-\Delta^2_{m'}(\vec{k}',\omega')}}\right], \quad (1)$$

where the kernels for the electron-phonon coupling are given by

$$F^{\pm}_{m\vec{k}\omega,m'\vec{k}'\omega'}=\int_0^\infty d\nu\sum_\lambda |g_{m'\vec{k}',m\vec{k},\lambda}|^2\delta[\nu-\omega_\lambda(\vec{k}'-\vec{k})]\Big\{[n(\nu)+f(-\omega')]\Big[\frac{1}{\omega+\omega'+\nu+i0^+}\mp\frac{1}{\omega-\omega'-\nu+i0^+}\Big]$$
$$\mp[n(\nu)+f(\omega')]\Big[\frac{1}{\omega-\omega'+\nu+i0^+}\mp\frac{1}{\omega+\omega'-\nu+i0^+}\Big]\Big\}. \quad (2)$$

Here $dS_{m\vec{k}}=k^2\,d\hat{\Omega}/[(2\pi)^3|\nabla_{\vec{k}}E_{m\vec{k}}|]$ is the unit of area on the Fermi surface of band m, and $f(\omega)=1/(e^{\beta\omega}+1)$ and $n(\nu)=1/(e^{\beta\nu}-1)$ are the Fermi and Bose functions, respectively.[16] The Coulomb pseudopotential is given by $\mu^*=N(0)U$, and $g_{m'\vec{k}',m\vec{k},\lambda}$ is the electron-phonon matrix element for phonons of frequency $\omega_\lambda(k-k')$ to scatter electrons from state $(m,\vec{k})$ to state $(m',\vec{k}')$.[15,17]

The quasiparticle density of states (DOS) $n_m^{(s)}(\vec{k},\omega)$ for a state of energy ω at the momentum $\vec{k}$ on the mth band at the Fermi surface is given by[16]

$$n_m^{(s)}(\vec{k},\omega)\equiv\mathrm{Re}\left[\frac{\omega}{\sqrt{\omega^2-\Delta_m^2(\vec{k},\omega)}}\right]. \quad (3)$$

To properly account for the complicated electronic structure of YBCO, the bands and matrix elements in Eqs. (1) were calculated by a self-consistent first-principles linear combination of atomic orbitals (LCAO) method using a nonorthogonal atomic basis of 47 orbitals. The calculated electronic structure agrees with other well-converged calculations to better than 10%. This LCAO calculation also provides the electron wave functions used to evaluate the matrix elements $g_{m'\vec{k}',m\vec{k},\lambda}$ of the electron-phonon interaction. Since both the LCAO band structure and the electron-phonon interaction are evaluated using a nonorthogonal tight-binding atomic basis, the ambiguity in the orthonormality encountered in the previous calculation[15] is absent here. The phonon frequencies and eigenvectors were computed using a shell model adopted by Humlicek *et al.*[18] that agrees well with neutron scattering data.

Since the electron states involving the electron-phonon interaction are near the Fermi surface, the energy dependence of the normal state electronic DOS was ignored in the calculation, but the anisotropy on the Fermi surface was retained. The momentum integrations in Eqs. (1) were done using a mesh of 72 points in the irreducible Brillouin zone. Computer memory and CPU time limited the calculation to this number of points, although previous experience indicates that a substantially larger number of points would not result in significant improvements. The calculation error was estimated at about 20% and must be considered when making a quantitative comparison with experimental data. The major computational error came from the nonorthogonal tight-binding fit to the electron-phonon interaction. But the main structure of the calculated quasiparticle spectrum is reliable and agrees with experimental results.

Equations (1) were solved by repeated iteration using a value of $\mu^*=0.1$ until the quasiparticle DOS calculated from Eq. (3) changed by less than 0.5% in a single step. When convergence was achieved, the average change in the gap function per interaction was less than 0.05 meV; the largest change was seen in the vicinity of the peak at $\omega\approx\Delta(k,\omega=0)$ where a change of about 0.25 meV occurred per iteration. We found that the solution converged most slowly for temperatures close to T_c, where about 50 iterations were needed to get a converged solution. The T_c value obtained from this calculation was 89 K and was in good agreement with that derived from a direct matrix diagonalization of the linearized gap equation on the imaginary axis.[15,19]

III. RESULTS

To compare our calculated DOS with the tunneling experiments, we note that in most experiments the anisotropic $\vec{k}$ dependence is not detected, so we have computed the effective tunneling DOS as a Fermi surface average using

$$n^{(s)}(\omega)=\sum_{m,\vec{k}} N_m^{(n)}(\vec{k})n_m^{(s)}(\vec{k},\omega)\Big/\sum_{m,\vec{k}} N_m^{(n)}(\vec{k}), \quad (4)$$

where $N_m^{(n)}(\vec{k})$ is the electronic density of states in the normal state for band m at $\vec{k}$ point on the Fermi surface and is obtained from the first-principles band structure.

The averaged quasiparticle DOS $n^{(s)}(\omega)$ we have found for YBCO is shown in Fig. 1 for temperatures of 0, 30, 60, 89, and 120 K. Figure 1(a) shows the density of states at 0 K. Because of the large variation in gap energies over the various pieces of the Fermi surface, the low temperature spectrum has very broad features. The density of states is zero

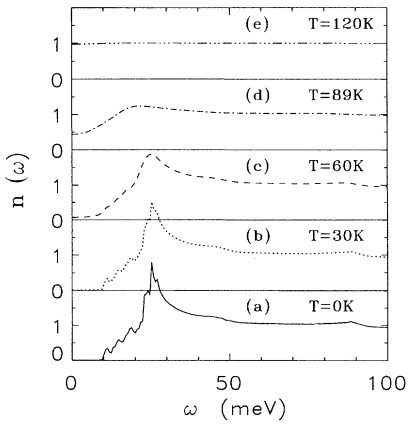

FIG. 1. The averaged isotropic quasiparticle DOS for YBCO at T = 0, 30, 60, 89, and 120 K.

below 9 meV. At about 25 meV there is a sharp peak which we attribute to the superconducting gap values of about 22 to 25 meV at some of the k points on the Fermi surface. We will discuss this in detail later when the k dependence of quasiparticle spectrum is discussed. At higher energy, there are minor features at about 47 and 88 meV that arise from the strong electron-phonon interaction and are related to the peaks of $\alpha^2F(\omega)$ at phonon energies of about 25 and 65 meV. We suspect for reasons discussed below that some of the fine structure in the low energy region may result from the use of a finite number of k points in the computation.

The density of states at 30 K, shown in Fig. 1(b), differs from that at 0 K only in the thermal smearing of some of the fine structure. Figure 1(c) shows that at 60 K, the fine structure in the region of 10 to 20 meV has been smoothed out, while the structure at 86 meV remains. This suggests that the fine structure at low energy may be a computational artifact, while the high energy features are intrinsic. In addition to a discernible drop in the magnitude of the gap, we now see some weight in the DOS at zero energy. This gapless behavior arises from the vanishing of the real part of gap function $\Delta(\vec{k},\omega)$ as $\omega\rightarrow 0$ and the rising of the imaginary part of the gap function at some points on the Fermi surface where the superconducting gap value (referred the value at T = 0 K) are relatively small compared to other k points. We will give a detailed discussion of exactly where in the Fermi surface this occurs below.

Figure 1(d) shows the quasiparticle DOS at the nominal transition temperature of 89 K. The quasiparticle DOS at $\omega = 0$ is about half of that of high energy. The real part of the gap function $\Delta(\vec{k},0)$ for all the k points on the Fermi surface become zero and the material is not superconducting. However, the energy gap function $\Delta(\vec{k},\omega)$ is still nonzero for $\omega>0$ on some of the bands. Furthermore, the dispersion in $\Delta(\vec{k},\omega)$ in the low energy region gives a large imaginary part $\mathrm{Im}[\Delta(\vec{k},\omega)]\approx\omega$. When this is included in Eq. (3) we find a quasiparticle DOS that is roughly half of the normal state DOS. This behavior is consistent with the structure seen experimentally in the tunneling spectrum of high-T_c superconductors at or slightly above T_c.[1–7,20–25] For example, the tunneling spectrum of $YBa_2Cu_3O_7$ reported by Gurvitch *et al.* and others,[1,7] has a sharp peak at about 24 meV which is very close to the sharp peak in our calculated quasiparticle DOS as in Fig. 1. The tunneling data show a systematic change with temperature and are not flat even above T_c. Similar behavior to what we calculate here for YBCO has also been seen in tunneling data on Bi-Sr-Cu-O systems.[21,2]

In order to make quantitative comparison with the experiments, we would need information on the energy dependence of the tunneling matrix element. This information may be extracted from measurements above 120 K, where the quasiparticle DOS shown in Fig. 1(e) appears flat. There is no remnant gap function $\Delta(\vec{k},\omega)$ on any of the branches of the Fermi surface. The small variation of the calculated curve from a flat line is primarily due to computational error, and gives an idea of the quality of the calculation. Thus one can see the effect of the frequency-dependent gap function in YBCO by taking the difference of the measured spectrum at low temperature from that of normal state.

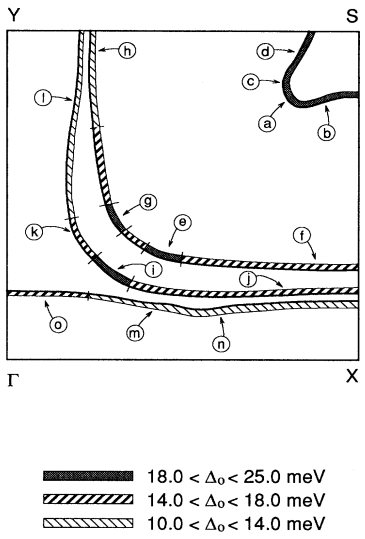

FIG. 2. The Fermi surface and the distribution of the superconducting gap values at $T = 0$ K for YBCO, with various points identified for later reference.

In order to show how the unusual features of the quasiparticle DOS shown in Fig. 1 can arise, we turn to a detailed examination of the variation of the quasiparticle DOS over the Fermi surface. The features that we will describe below should be visible in high-resolution angle-resolved photoemission spectroscopy (ARPES). There are four bands crossing the Fermi energy in YBCO, yielding four pieces of Fermi surface. We will present the quasiparticle DOS $n^{(s)}(\vec{k},\omega)$ at selected k points on each of the four pieces of the Fermi surface. The points are labeled in Fig. 2.

Figure 3 displays the quasiparticle DOS at $T=0$ for these selected k points. Figure 3(a) shows the spectrum for the four k points that are on the small piece of the Fermi surface around the S point. Since all four k points have quite large energy gap values of about 22 to 25 meV, we conclude that the gap on this piece of the Fermi surface is s wave with little anisotropy. The small features at 47 and 88 meV are related to the peaks at about 25 and 65 meV in $\alpha^2F(\omega)$. Figure 3(b) shows the DOS of four k points (labeled e-h on Fig. 2) on the second piece of Fermi surface away from S point, this band being mainly derived from orbitals in the Cu-O plane. These four points have quite different gap values, with point e having a gap of 25 meV, similar to that of Fig. 3(a), but all show characteristic BCS behavior in the DOS. The results for the third piece of Fermi surface away from the S point (points i, j, k, and l) are shown in Fig. 3(c), and are also consistent with anisotropic, but essentially s-wave, pairing. Figure 3(d) shows the results for the three k points (m, n, o) on the fourth piece of Fermi surface which is close to the Γ-X line. While the gap value of point o is about 18 meV, the other two points have considerably smaller gaps of about 9 to 13 meV. The quasiparticle DOS at $T=30$ K is shown in Fig. 4, and is essentially the same as at $T=0$ except for the decrease in the height of the peak at the gap due to thermal smearing.

At $T=60$ K, the calculated results are shown in Fig. 5,

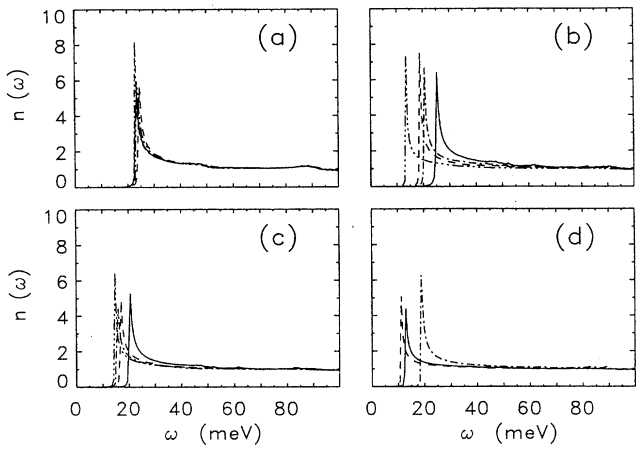

FIG. 3. The quasiparticle DOS for $T = 0$ K. (a) DOS on four $\vec{k}$ points on a piece of Fermi surface around the S point in the Brillouin zone. (b) DOS on the selected four $\vec{k}$ points on the second piece of Fermi surface away from the S point; the solid line for point e, dashed line for point f, dashed-dot line for point g, and dashed-dot-dot-dot line for point h. (c) Four $\vec{k}$ points on the third piece of Fermi surface away from the S point; the solid line for point i, dashed line for point j, dashed-dot line for point k, and dashed-dot-dot-dot line for point l. (d) Three $\vec{k}$ points on the Fermi surface near the Γ-X line; the solid line for point m, dashed line for point n, dashed-dot line for point o. All the symbols (e, f, g, h, i, ...) used here are the same as in Fig. 2.

which clearly show a change from the results in Fig. 3 and Fig. 4. The peaks in the DOS become much smaller, continuing the trend seen in Fig. 4, and all the gaps tend to decrease somewhat. Interestingly, at some points on the Fermi surface the gap collapses entirely, leading to a nonzero quasiparticle density of states at zero energy. This can be seen in Figs. 5(b), 5(c), and 5(d). However, this gaplessness clearly occurs only on parts of the Fermi surface, with other points retaining a nonzero gap.

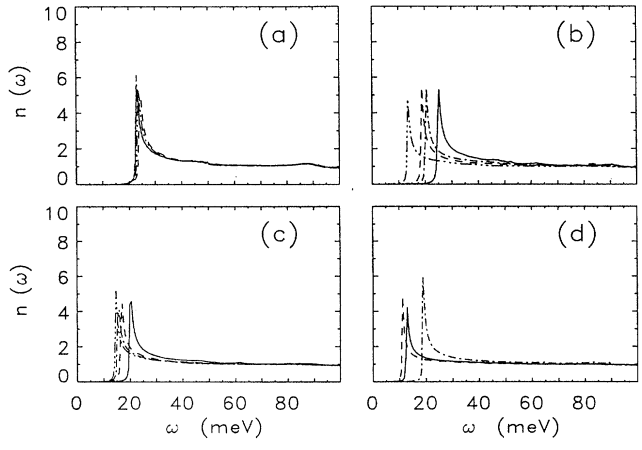

FIG. 4. Quasiparticle DOS at a temperature of 30 K. All the selected $\vec{k}$ points and line styles are the same as in Fig. 3.

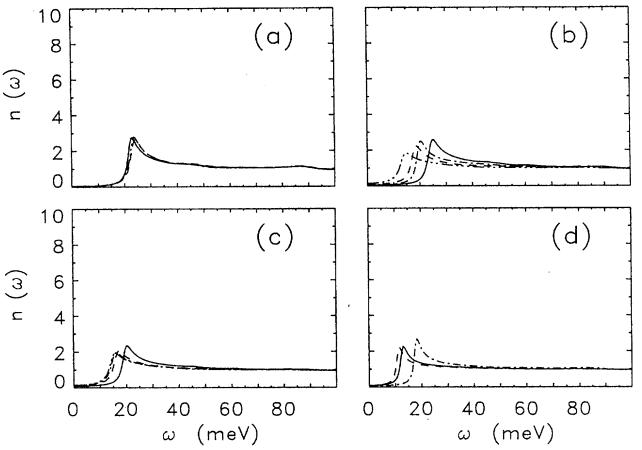

FIG. 5. Quasiparticle DOS at 60 K. All the selected $\vec{k}$ points and line styles are the same as in Fig. 3.

This "gapless s-wave" superconducting state appears at first sight to be d-wave pairing in disguise. We have checked that the gap does indeed vanish, but since we impose the full symmetry of the crystal on the gap function and see no sign change in the irreducible portion of the Brillouin zone where we calculate, the gap does not change sign anywhere on the Fermi surface. Thus this behavior is not the same as d-wave pairing where the gap should change sign. Gaplessness in an s-wave superconductor usually arises from magnetic impurities or other pair-breaking mechanism and involves the disappearance of the gap everywhere on the Fermi surface.[26] The gapless s-wave state we see arises from the complicated electron-phonon coupling and band structure that we have used. Computational limitations prevented us from examining the possibility that the gap had d-wave component with the same accuracy as our s-wave calculation. We did perform a less detailed calculation for the gap at zero temperature using fewer points but including the full Brillouin zone gap

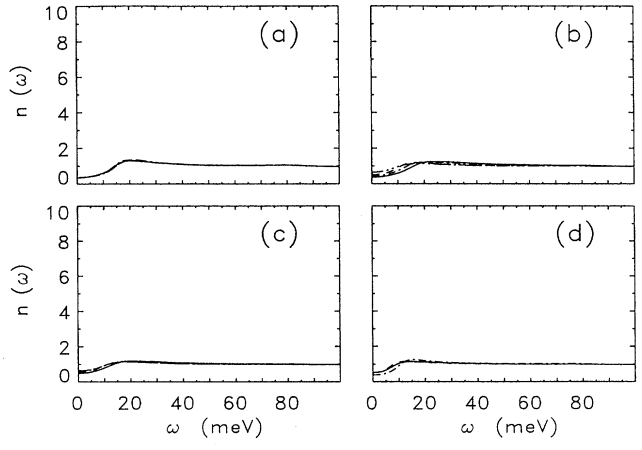

FIG. 6. Quasiparticle DOS at $T_c = 89$ K. All the selected $\vec{k}$ points and line styles are the same as in Fig. 3.

and found no evidence for a d-wave component. The possibility of d-wave pairing will be explored in a future publication.

Figure 6 shows the quasiparticle DOS at a temperature very close to T_c (T = 89 K) using the same k points as in Fig. 3. At all of these points the real part of the gap function $\Delta(\vec{k},0)$ has vanished. The imaginary part of the gap function is quite large at low frequencies. The values of the imaginary part of the gap function at all the k points are larger than the excitation energy ω. However, the real part of the gap function $\Delta(\vec{k},\omega)$ for $\omega>0$ is not zero for all the k points on the Fermi surface. Some minor structures in the low energy of the spectra still can be seen. Thus even above T_c, we have a kind of "transient" superconductivity existing at finite frequency on some parts of the Fermi surface that will affect the tunneling DOS. While this behavior in normal superconductors (with no noticeable gap structure) is what gives rise to the fluctuation conductivity, in these strong-coupling systems we also see the effect in the tunneling density of states. These explain the tunneling DOS results in Fig. 1 and also the tunneling experiments at or slightly above T_c.[1,7]

IV. CONCLUSIONS

We have calculated the quasiparticle spectrum for YBCO and compared with experimental results. We find that the quasiparticle DOS is strongly momentum and band dependent. The broad structure in the tunneling data can be understood by solving the anisotropic, several-band version of the Eliashberg equations using electronic bands, phonon dispersion, and electron-phonon interactions derived from realistic calculations. The sharp peak seen at about 25 meV in the tunneling spectrum is reproduced in this calculation. We also found weaker features at about 45 meV and 90 meV that are related to particular features in the electron-phonon interaction. The broad foot in low energy region seen at low temperatures is related to the wide distribution of gaps on the different bands including some parts of the Fermi surface where the gap vanishes completely. The wide variation in gap energies and the persistence of the gap at nonzero frequency above T_c also explains the structure in the tunneling data near T_c.

These gapless regions are different from the nodes that are indicative of d-wave pairing, because there is no sign change of the gap in our calculations [$\mathrm{Re}\,\Delta(\vec{k},\omega\rightarrow 0)\geq 0$]. However, they affect the density of states in the same way as d-wave pairing and will thus lead to similar power-law behavior (except at very low temperatures) in the temperature dependence of the NMR relaxation[27] and other quantities[28–30] depending primarily on the quasiparticle DOS. Other experimental results claimed as evidence for d-wave pairing[31,32] should be reexamined to see if they can be explained with an anisotropic, gapless s-wave pairing state.

While we have accounted for many of the features seen in the tunneling data, we still cannot account for the zero bias anomaly or the curvature in the normal state DOS. It is perhaps here that the strong electron correlations postulated in some theories plays a crucial role. In our calculations we only see gaplessness arising from structure in the electron-phonon interaction above a certain temperature. It is possible that many-body effects or localized magnetic moments combined with strong anisotropy of the pairing interaction[33] within the plane could extend the gapless behavior down to zero temperature.

ACKNOWLEDGMENTS

The authors are grateful to Phil Adams for valuable discussions. This research work was supported by the National Science Foundation under Grant No. DMR 91-20166.

*Deceased.

[1] M. Gurvitch, J. M. Valles, Jr., A. M. Cucolo, R. C. Dynes, J. P. Garno, L. F. Schneemeyer, and J. V. Waszczak, Phys. Rev. Lett. **63**, 1008 (1989); A. M. Cucolo, R. C. Dynes, J. M. Valles, Jr., and L. F. Schneemeyer, Physica C **179**, 69 (1991).

[2] T. Ekino and J. Akimitsu, Phys. Rev. B **40**, 6902 (1989); **42**, 8049 (1990); J. Supercond. **7**, 367 (1994).

[3] T. Becherer, C. Stolzel, G. Adrian, and H. Adrian, Phys. Rev. B **47**, 14 650 (1993).

[4] E. Polturak, G. Koren, D. Cohen, and E. Aharoni, Phys. Rev. B **47**, 5270 (1993).

[5] I. Iguchi and T. Kusumori, Phys. Rev. B **46**, 11 175 (1992).

[6] R. B. Laibowitz, R. P. Robertazzi, R. H. Koch, A. Kleinsasser, J. R. Kirtley, J. M. Viggiano, R. L. Sandstrom, and W. J. Gallagher, Phys. Rev. B **46**, 14 830 (1992).

[7] H. T. Chen and T. T. Chen, Physica C **213**, 151 (1993).

[8] J. Ma, C. Quitmann, R. J. Kelley, H. Berger, G. Margaritondo, and M. K. Onellion, Science **267**, 862 (1995).

[9] R. Liu, B. W. Veal, A. P. Paulikas, J. W. Downey, P. J. Kostic, S. Fleshler, U. Welp, C. G. Olson, X. Wu, A. J. Arko, and J. J. Joyce, Phys. Rev. B **46**, 11 056 (1992).

[10] N. Schroeder, R. Böttner, S. Ratz, E. Dietz, U. Gerhardt, and Th. Wolf, Phys. Rev. B **47**, 5287 (1993).

[11] J. C. Campuzano *et al.*, Phys. Rev. Lett. **64**, 2308 (1990).

[12] J. G. Tobin, C. G. Olson, G. Gu, J. Z. Liu, F. R. Solal, M. J. Fluss, R. H. Howell, J. C. O'Brien, H. B. Radousky, and P. A. Sterne, Phys. Rev. B **45**, 5563 (1992).

[13] Y. Sakisaka *et al.*, Phys. Rev. B **39**, 9080 (1989).

[14] Z. X. Shen *et al.*, Phys. Rev. Lett. **70**, 1553 (1993).

[15] G. L. Zhao and J. Callaway, Phys. Rev. B **49**, 6424 (1994); **50**, 9511 (1994).

[16] J. P. Carbotte, Rev. Mod. Phys. **62**, 1027 (1990); J. P. Carbotte, in *Anisotropy Effects in Superconductors*, edited by H. W. Weber (Plenum, New York, 1977), p. 183.

[17] C. M. Varma and W. Weber, Phys. Rev. Lett. **39**, 1094 (1977).

[18] J. Humlicek, A. P. Litvinchuk, W. Kress, B. Lederle, C. Thomsen, M. Cardona, H. U. Habermeier, J. E. Trofimov, and W. Konig, Physica C **206**, 345 (1993).

[19] P. B. Allen and B. Mitrovic, in *Solid State Physics*, edited by H. Ehrenreich and D. Turnbull (Academic, Orlando, 1982), Vol. 37, p. 1.

[20] H. J. Tao, A. Chang, F. Lu, and E. L. Wolf, Phys. Rev. B **45**, 10 622 (1992).

[21] T. Walsh, J. Moreland, R. H. Ono, and T. S. Kalkur, Phys. Rev. B **43**, 11 492 (1991).

[22] S. I. Vedeneev, A. G. M. Jansen, P. Samuely, V. A. Stepanov, A. A. Tsvetkov, and P. Wyder, Phys. Rev. B **49**, 9823 (1994).

[23] M. Lee, D. B. Mitzi, A. Kapitulnik, and M. R. Beasley, Phys. Rev. B **39**, 801 (1989).

[24] A. I. Akimenko, G. Goll, H. v. Lohneysen, and V. A. Gudimenko, Phys. Rev. B **46**, 6409 (1992).
[25] A. M. Cucolo, R. D. Leo, P. Romano, B. Dabrowski, D. G. Hinks, and P. G. Radaelli, Phys. Rev. B **50**, 10 397 (1994).
[26] K. Maki, in *Superconductivity*, edited by R. D. Parks (Marcel Dekker, New York, 1969), p. 1037.
[27] J. Ohsugi, Y. Kitaoka, M. Kyogaku, K. Isihida, K. Asayama, and T. Ohtani, J. Phys. Soc. Jpn. **61**, 3054 (1992).
[28] S. E. Stupp and D. M. Ginsburg, in *Physical Properties of High Temperature Superconductors III*, edited by D. M. Ginsburg (World Scientific, Singapore, 1991).
[29] R. C. Yu, M. B. Salamon, and W. C. Lee, Phys. Rev. Lett. **69**, 1431 (1990).
[30] W. N. Hardy, D. A. Bonn, D. C. Morgan, R. Liang, and K. Zhang, Phys. Rev. Lett. **70**, 3999 (1993).
[31] D. A. Wollman, D. J. van Harlingen, W. C. Lee, D. M. Ginsberg, and A. J. Leggett, Phys. Rev. Lett. **71**, 2134 (1993).
[32] T. Hanaguri, T. Fukase, Y. Koike, I. Tanaka, and H. Kojima, Physica (Amsterdam) **165&166B**, 1449 (1990); K. Takanaka and K. Kuboya, Phys. Rev. Lett. **75**, 323 (1995).
[33] V. Kresin and S. A. Wolf, Phys. Rev. B **51**, 1229 (1995).